Published in final edited form as:

Nat Photonics. 2019 June ; 13(6): 412–417. doi:10.1038/s41566-019-0396-4.

Stimulated Raman Excited Fluorescence Spectroscopy and Imaging

Hanqing Xiong[†], **Lixue Shi**[†], **Lu Wei**, **Yihui Shen**, **Rong Long**, **Zhilun Zhao**, **Wei Min**[*]

Department of Chemistry, Columbia University, New York, NY 10027, USA

Abstract

Powerful optical tools have revolutionized science and technology. The prevalent fluorescence detection offers superb sensitivity down to single molecules but lacks sufficient chemical information[1-3]. In contrast, Raman-based vibrational spectroscopy provides exquisite chemical specificity about molecular structure, dynamics and coupling, but is notoriously insensitive[3-5]. Here we report a hybrid technique of Stimulated Raman Excited Fluorescence (SREF) that integrates superb detection sensitivity and fine chemical specificity. Through stimulated Raman pumping to an intermediate vibrational eigenstate followed by an upconversion to an electronic fluorescent state, SREF encodes vibrational resonance into the excitation spectrum of fluorescence emission. By harnessing narrow vibrational linewidth, we demonstrated multiplexed SREF imaging in cells, breaking the "color barrier" of fluorescence. By leveraging superb sensitivity of SREF, we achieved all-far-field single-molecule Raman spectroscopy and imaging without plasmonic enhancement, a long-sought-after goal in photonics. Thus, through merging Raman and fluorescence spectroscopy, SERF would be a valuable tool for chemistry and biology.

To merge the advantages from both worlds of Raman and fluorescence, our idea is to develop a new hybrid spectroscopy by encoding vibrational features onto the fluorescence spectrum. Before we reach the optimized design, we have gone through a series of theoretical consideration and experimental refinement (Fig. 1). While linear fluorescence spectroscopy excites the electronic transition directly (Fig. 1a), nonlinear fluorescence excitation can employ one or more virtual states as intermediates, thus potentially probing more states (Fig. 1b). However, conventional nonlinear fluorescence still lacks chemical specificity, owing to the extremely short-lived virtual states (i.e., large energy uncertainty). We reason that, if a long-lived vibrational eigenstate with a well-defined energy level can mediate a multiphoton fluorescence excitation process, the intermediate vibrational information can then be encoded into the fluorescence excitation spectrum. Indeed, such double resonance spectroscopy have been explored decades ago in which an infrared (IR)

---

[*]Corresponding author. wm2256@columbia.edu.

[†]These authors contribute equally to this work

Author Contributions: H.X. and L.S. collected and analyzed all the data; H.X. designed and constructed the instrument with the help of L.S. and Z.Z. under the guidance of W.M.; L.W. and Y.S. contributed to the early phase of the spectroscopy project; R.L. performed chemical synthesis; W.M. conceived the concept; H.X., L.S. and W.M. wrote the manuscript with the input from all authors.

Methods, along with any additional Supplementary display items, are available in the online version of the paper; references unique to these sections appear only in the online paper.

pulse excites an intermediate vibrational transition followed by a visible pulse to excite the fluorescence (Fig. 1c)[6]. Despite being a powerful approach to investigate vibrational dynamics of chromophores[7,8], the strong IR absorption in water and poor spatial resolution are intrinsically unfavorable for applications in biological systems. Moreover, the reported sensitivity is still several orders away from single molecules.

Considering stimulated Raman scattering (SRS) is complementary to IR excitation by offering much higher spatial resolution and avoiding water absorption, we take a different approach, stimulated Raman excited fluorescence (SREF), by harnessing two beams (pump and Stokes) to coherently populate the intermediate vibrational state via SRS and a third probe beam to up-convert the vibrational population to the electronic excited state for subsequent fluorescence (Fig. 1d). Unlike conventional fluorescence spectroscopy (Fig. 1a&b), SREF is a Raman-mediated three-photon process, thus its excitation spectrum, by tuning ω_p -ω_s, should map out vibrational information of electronic ground state. Figure 1e illustrates the microscope setup (details in Methods and Supplementary Fig. 1). Briefly, temporally and spatially overlapped pump (ω_p tunable) and Stokes (ω_s, 1031.2-nm) picosecond pulse trains are focused by a high N.A. objective to perform SRS excitation. The pump pulse (either through one-photon or two-photon) also plays the role of probe pulse (green line or red dash line) for excitation to the electronic excited state for fluorescence emission. Backward fluorescence is then detected by a small-area avalanche photodiode (APD) with confocal detection. Both the reflected laser beams and the coherent anti-Stoke Raman scattering (CARS) signal[9] are completely blocked by proper filter sets.

However, our initial attempt on a coumarin dye (SRS excitation of C=C mode followed up by two-photon excitation to the fluorescent state) was unsuccessful without detecting any vibrational feature by tuning ω_p -ω_s. We found that, even with a quantum amplification up to 10^8 achieved under modern SRS microscopy[10], the effective SRS excitation cross sections are still less than 10^{-20} cm^2 for typical chromophores including coumarin, resulting in much less efficient vibrational pumping rate compared to the rapid vibrational relaxation (sub-picosecond) of molecules in condensed phases[7]. As a result, this SREF pathway is easily overwhelmed by other competing processes such as two-photon fluorescence background, which was observed in our attempt on coumarin and previous unsuccessful trial on perylene dye[11].

We note that the above unsuccessful SREF attempt should be associated with SRS being operated in the non-resonance region (Fig. 1d), with the pump laser energy, ω_p, being well below the molecular absorption peak energy, ω_{abs}. It is well known that Raman cross section of electronically coupled vibrational modes can be enhanced up to 10^7 when ω_p is brought close to ω_{abs}[12]. We then revisited the SREF approach aiming to significantly enhance the SRS pumping rate under the close electronic resonance (Fig. 1f). A near-IR dye ATTO 740 (ω_{abs}, 760-nm in DMSO) and its nitrile mode (Raman peak at 2227 cm^{-1}) was used in our second attempt (Supplementary Fig. 2a). The SREF excitation spectra of ATTO 740 were acquired by tuning ω_p across the nitrile Raman peak. Although a strong SRS peak was detected as stimulated Raman loss of the pump beam, no vibrational feature was observed on the fluorescence excitation spectrum. Apparently, too-close resonance condition of SRS

is unavoidably accompanied by a strong anti-Stokes fluorescence background directly excited by the pump beam, which can easily overwhelm the SREF signal.

We then realize that, linear absorption cross section (which determines the anti-Stokes fluorescence background) can decay faster than that of (pre)resonance Raman scattering cross section (which determines the SRS pumping rate) as a function of pump detuning of ω_{abs} - ω_p[13]. Hence, we hypothesize that a proper pump detuning might help attenuate the anti-Stokes fluorescence background and, at the same time, largely retain the desired SREF signal. As the third attempt, we experimented on the C=C skeletal mode (Raman peak at 1640 cm^{-1}) for ATTO 740 (Supplementary Fig. 2b), which corresponds to a larger pump detuning than that of nitrile mode (Fig. 1g). Indeed, with the anti-Stokes fluorescence background decreasing by ~10 folds than that of the close-resonance case (Supplementary Fig. 2a, b, blue dash curves), an obvious Raman-like peak was detected on top of the broad fluorescence excitation spectrum (Supplementary Fig. 2b, blue line in right column). Hence, the above two tests (Supplementary Fig. 2) on the same ATTO 740 dye clearly support our strategy of retrieving SREF peak by proper electronic pre-resonance.

To demonstrate SREF as a general approach, we adopted a popular dye Rhodamine 800 (Rh800) (Fig. 2a) with higher fluorescence quantum yield than ATTO 740 and better collection efficiency due to its bluer emission. Rh800 bears a conjugated nitrile (C≡N) moiety with a distinct Raman peak at 2236 cm^{-1} (Fig. 2b)[14]. When ω_p -ω_s is tuned to match the C≡N vibration, SRS is operating in the region of electronic pre-resonance (ω_p around 838 nm, ω_{abs} ~ 700 nm), and the total energy (ω_p - ω_s) + ω_p reaches its ω_{abs} (Fig. 2a). We then obtained the SREF excitation spectrum by sweeping ω_p across the C≡N resonance with 500 nM Rh800 solution. Remarkably, a pronounced Raman-like peak has emerged at 2236 cm^{-1} within the fluorescence excitation spectrum (Fig. 2c, solid line). Both its position and width are consistent with the corresponding SRS peak (Fig. 2b), proving its vibrational origin. As a negative control, the pump beam alone generates one-photon anti-Stokes fluorescence from thermally excited vibrational population (Fig. 2c, blue dash line; Supplementary Fig. 3a), and the Stokes beam alone mainly leads to two-photon excited fluorescence (Fig. 2c, red dash line; Supplementary Fig. 3b).

We further characterized SREF spectroscopy. First, the time-delay dependence fits well with the cross-correlation profile of pump and Stokes pulses (Fig. 2d). Second, the laser power dependence is linear to both pump and Stokes beams (Fig. 2e, (f), since the up-conversion step to the fluorescent state is already saturated with our pulsed probe (pump) laser[15] (see Methods and Supplementary Fig. 4). Third, general SREF detectability is demonstrated on more molecules in both fingerprint region (double bond) and cell-silent region (triple bond) (Supplementary Fig. 5). Finally, we confirmed the linear concentration dependence with a superb sensitivity readily down to 10 nM (Fig. 2g). The corresponding SREF signal is extrapolated to be 2~3 photons per ms at the single-molecule-equivalent concentration (~8 nM). Relatively poorer detection sensitivity is obtained for C=C mode in ATTO740 (owing to its poorer fluorescence quantum yield and collection efficiency) (Supplementary Fig. 2c).

It is constructive to theoretically analyze the SREF signal of Rh800. A vibrational excitation rate of 8×10^3 per millisecond (ms) is estimated from Fig. 2b for a single C≡N bond of

Rh800 under the excitation of merely 12-mW pump beam and 13-mW Stokes beam (see Methods). For SRS detection whose sensitivity is limited by laser shot noise (about 7×10^6 photons per ms for the pump beam), 1,000 Rh800 molecules are required to overcome the shot noise. In contrast, SREF can circumvent the overwhelming laser background by upconverting some of the vibrational population to electronic-excited state for subsequent fluorescence detection. In addition to electronic pre-resonance, how to optimize the upconversion efficiency is another key. Our analysis suggests that, under our experimental condition, the upconversion efficiency is almost totally determined by the competition between SRS pumping and the relaxation of vibrational excited state (see Methods). We noted that vibrational relaxation often occurs very fast in polyatomic molecules: a vibrational lifetime of 0.5 ps is estimated by considering a predominately lifetime-broadened vibrational linewidth (~ 11 cm^{-1} for C≡N in Rh800)[7]. That is why 2-ps pulses were chosen to be short enough to compete favorably with vibrational relaxation yet long enough to maintain the fine spectral selectivity. In contrast, an inefficient pulse width of 5-ns was used in the previous unsuccessful attempt[11]. Numerically, we modeled the SREF process with a three-level rate equation, and obtained 20% upconversion efficiency, close to the result from steady-state approximation (see Methods and Supplementary Fig. 4). This corresponds to a SREF excitation rate about 1.6×10^3 per ms. Considering the 16% fluorescence quantum-yield[16] and an overall 2% microscope fluorescence collection, a moderate signal of 5 photons per ms is theoretically estimated from a single Rh800 molecule, which agrees well with experimental measurement (extrapolated to ~8 nM in Fig. 2g).

SREF combines the desirable properties of chemical specificity and superb sensitivity, thereby going beyond the standard fluorescence and Raman spectroscopy. To showcase the exquisite vibrational selectivity of SREF, we synthesized a set of new isotopologues for Rh800 containing isotopically-edited nitrile moiety (Fig. 3a, $^{12}C\equiv^{15}N$, $^{13}C\equiv^{14}N$ and $^{13}C\equiv^{15}N$; synthesis in Supplementary Information). As expected, the absorption and emission spectra are identical among these isotopologues, preventing their spectral separation by standard fluorescence techniques (Fig. 3b). In contrast, spectrally well-resolved SREF peaks from C≡N vibrations can be successfully acquired for four isotopologues (Fig. 3c and Supplementary Fig. 6), in agreement with corresponding Raman peak positions[14] (Fig. 3c, bottom, dashed).

By leveraging the fine vibrational specificity, we then demonstrate multiplexed SREF imaging. There is increasing demand for simultaneously imaging a large number of molecular targets in complex systems[17]. However, due to the limited chemical specificity, fluorescence microscopy exhibits a fundamental “color barrier”: in practice, no more than 5 fluorescent dye can be simultaneously imaged[18]. In our multiplexed SREF imaging, a single SREF image is obtained by sample raster scanning for a given ω_p (see Methods); a stack of hyperspectral images is then acquired by sweeping ω_p. As a proof of concept, living *E.coli* cells (Fig. 3d), each stained with one of the four Rh800 isotopologues and then mixed together, could be unequivocally resolved by the detected SREF peak (Fig. 3e) and assigned back to the corresponding Rh800 isotopologues (Fig. 3f). Thus, when coupled with newly developed palettes of vibrational probes[17], multiplexed SREF imaging can break the “color barrier” of fluorescence and hold the promise for super-multiplex optical microscopy.

We now demonstrate the first all-far-field vibrational imaging of single molecules at room temperature. We note that previous single-molecule Raman spectroscopy are only possible in the optical near field with the help of strong plasmonic enhancement[5,19-22]. Electronic resonance on light-absorbing chromophores is also indispensable for nearly all single-molecule surface-enhanced Raman spectroscopy: detecting single-molecule non-resonant molecules is extremely rare. Nonetheless, the strict reliance on close contact to metallic nanostructures (angstrom level precision) has limited the applicability of these near-field techniques in vast chemical and biological systems[23]. In retrospect, single-molecule fluorescence spectroscopy made its major impact in chemistry and biology after it transitioned from near-field to far-field. In light of this, single-molecule far-field Raman spectroscopy would have potential to impact many areas where metallic nanostructures are inaccessible or undesired.

For imaging single molecules in the far field, we followed standard sample preparations for embedding Rh800 in PMMA film[24] and validated the spectroscopic preservation using absorption, fluorescence and SREF spectra of Rh800 isotopologues (Fig. 4a, b and Supplementary Fig. 7). To assist locating and confirming individual molecules, a 660-nm continuous wave laser was used for one-photon fluorescence (details in Methods and Supplementary Fig. 1). Single-molecule distribution could be evidenced by abrupt photobleaching during raster scanning (half-moon pattern in Fig. 4c), occasional blinking, and single-step beaching time traces (Supplementary Fig. 8). We next acquired single-molecule SREF spectral images by sweeping ω_p across the vibrational resonance of C≡N in Rh800. Consistently more pronounced signal is observed at the on-resonance frequency for multiple molecules within the same field-of-view (Fig. 4d, e), as well as in repetitive pump scans over the same molecule (Fig. 4f, g). The peak position, shape and line-width all resemble the bulk SREF measurement, confirming the vibrational resonance (Fig. 4d-i). Quantitatively, about 4 photons per ms were detected from the brightest pixel from on-resonance images (Supplementary Fig. 9), comparable to the solution measurement. The single-molecule identity and its survival are further confirmed by additional 660-nm-excited fluorescence following SREF series and subsequent single-step photobleaching.

Such ultimate sensitivity is extendable to Rh800 isotopologues that are vibrationally distinct but electronically identical (Fig. 4h, i). By sweeping ω_p across the corresponding vibrational resonance, sharp SREF image contrasts were clearly observed at the expected Raman shifts for both $^{12}C{\equiv}^{15}N$ (2207 cm^{-1}) and $^{13}C{\equiv}^{14}N$ (2183 cm^{-1}) (Fig. 4h, i). Such fine chemical specificity at the single-molecule level would be extremely difficult, if not impossible, to be achieved by room-temperature fluorescence spectroscopy or absorption spectroscopy[2,25-28]. We further confirmed Raman selectivity of single-molecule SREF spectral images by conducting statistical tests over 61 complete image sets. For each set, we performed student's *t*-test between on-resonance signals and two adjacent off-resonance signals respectively, as well as between the two off-resonance channels (Fig. 4j, Supplementary Table 1). In most sets (53 out of 61), the on-resonance signals are statistically higher than off-resonance backgrounds ($p<0.05$). In contrast, no significant difference can be found between the two off-resonance channels. Interestingly, the signal-to-background ratios (on/off ratio) (Fig. 4k) show a broad distribution, which is likely originated from random orientations of individual Rh800 within PMMA film and the possible mismatch of dipole

moments between SREF and two-photon fluorescence (Supplementary Fig. 10). To the best of our knowledge, this is the first all-far-field Raman spectroscopy of single molecules[29,30].

In this work, we have integrated both the desired chemical selectivity and the superb sensitivity into a new Raman-mediated multiphoton fluorescence process of SREF. Different from previous attempt[11], electronic pre-resonance is devised and upconversion efficiency is optimized to ensure successful SREF detection above competing backgrounds. Agreement was found between theory (see Methods) and experiments for Rh800 and its isotopologues. Clear SREF spectroscopy of different Raman modes were recorded in several other dyes in both fingerprint region and cell-silent region (Fig. 3c, Supplementary Fig. 2, 5), supporting its general applicability. Most notably, single-molecule Raman spectroscopy and imaging are achieved at optical far-field (Fig. 4), bypassing the need of plasmonic enhancement. This would have profound implications, in light of the revolutionary impact of far-field single-molecule fluorescence spectroscopy. Besides spectroscopic applications, SREF has also great potential for biological imaging. Owing to its superior detection sensitivity than SRS (by about 100 times), multiplexed SREF would provide a more sensitive technique for super-multiplex vibrational imaging[17]. With the single-molecule imaging capability, localization-based methods would enable super-resolution vibrational imaging.

Further technical improvement would promise even higher signals and richer spectral information. For example, utilizing fluorophores with higher quantum yields (only 16% for Rh800 and 10% for ATTO740) could result in much brighter SREF signal; a more sophisticated laser source with both tunable pump and Stokes beams and ideally a separate probe beam could allow more flexible excitation control, enabling SREF investigation of many more molecules across the wide spectrum.

Methods

System configuration of lasers and microscope.

A comprehensive experimental scheme is shown in Supplementary Fig. 1. A picoEmerald S (Applied Physics & Electronics, Inc.) system was used to provide synchronized Stokes beam and pump beam for stimulated Raman scattering (SRS) and stimulated Raman excited fluorescence (SREF) measurements. The fundamental 1031.2 nm IR fiber laser (2-ps pulse width and 80-MHz repetition rate, 0.5-nm FWHM bandwidth) is adopted as our Stokes beam. A part of the IR laser was frequency-doubled to synchronously seed the OPO system and produce a tunable pump beam (2-ps pulse width, 0.5-nm FWHM bandwidth). The idler beam was blocked. All beams are linear polarized in the same direction. Pump and Stokes were expanded and coupled into an Olympus IX71 microscope to overfill the back pupil of objective for diffraction-limited-resolution imaging. A 60X water immersion objective (UPLSAPO, 1.2 N.A., Olympus) was used for all measurements. Two raster scanning methods were used for imaging: stage scanning for single molecule imaging and laser scanning for living cell imaging. Stage-scan was achieved with a XY piezo stage (P545, Physik Instrumente); laser scanning was achieved by a standard 2D-galvanometer (GVSM002, Thorlabs). All imaging scanning and data acquisition were controlled by home-written LabVIEW programs.

For SRS (stimulated Raman loss, SRL) detection, the Stokes beam was modulated at 20-MHz by an electro-optical modulator (EOM) to achieve shot-noise limited detection. The forward-going pump and Stokes beams after samples were collected by a high NA IR-coated oil condenser (1.4 NA, Olympus), which is aligned by Köhler illumination. A high-speed large-area silicon PIN photodiode (S3590-09, Hamamatsu) was used as the detector. A high OD bandpass filter (ET890/220m, Chroma) was placed in front of the photodiode to block the Stokes beam completely and transmit the pump beam. The photodiode was reversed biased by 64 V from a DC power supply to increase both the saturation threshold and response bandwidth. Signal output of the photodiode was then sent to a fast look-in amplifier (HF2LI, Zurich Instruments) for signal demodulation. The demodulated signal was digitalized by a NI card (PCI-6259, NI) driven by our home-written LabVIEW program.

In SREF, the Stokes laser is not modulated. For SREF detection of Rh800 and MARS dyes (both nitrile bond and C=C bond), pump and Stokes beams pass through a dichroic mirror (FF825-SDi01, Semrock) to excite the molecules, and the backward fluorescence is then detected. Two bandpass filters (FF01-709/167-25, Semrock) each with OD greater than 6 are used to block the reflected laser beams, and another bandpass filter (FF01-735/28-25, Semrock) with OD greater than 7 is adopted for completely blocking the CARS background. For SREF detection of ATTO740 C=C bond, the corresponding dichroic mirror is FF825-SDi01 (Semrock) and the filters include two bandpass filters (FF01-819/44-25, Semrock). For SREF detection of ATTO740 nitrile bond, the corresponding dichroic mirror is FF825-SDi01 (Semrock) and the filters include two bandpass filters (FF01-709/167-25, Semrock) for blocking of reflected laser beams, and another bandpass filter (FF01-785/62-25, Semrock) for completely blocking of CARS background. A high quantum-yield (~70% at 700-nm) single photon counting module (SPCM) (SPCM-NIR-14-FC, 70-cps dark counts, Excelitas) was used to detect fluorescent emission for general measurements, and a similar quantum-yield SPCM but with much lower dark counts (SPCM-AQRH-16-FC, 7-cps dark counts, Excelitas) was used for single-molecule SREF imaging presented in Fig. 4. The 100-μm active APD diameter forms a loose confocal configuration for detection and imaging.

For parallel single-molecule fluorescence detection, an additional 660-nm CW laser (Coherent) was coupled into the microscope. A quarter wave plate was used to transform the linear polarization to circular polarization. For 660-nm CW laser excited fluorescence detection of Rh800, laser pass through a dichroic mirror (690dcxr, Chroma), and fluorescence is collected after two bandpass filters (FF01-795/150-25, Semrock; FF01-747/33-25, Semrock).

Physical model for SREF signal estimation.

Since the electronic coherence dies out in condensed phase at room temperature within tens of femtoseconds[31], and our SRS excitation rate is much slower than the decay rate of vibrational coherence[32], it is feasible to model the SREF process by rate equations of a three-level system[33,34]. The energy-level diagram is shown in Supplementary Fig. 4a. N_1, N_2 and N_3 represent the population on the corresponded states. W_{12} is the epr-SRS excitation rate, w_{21} is the vibrational relaxation rate for targeted vibrational mode, W_{23} is the probe excitation rate from vibrational excited state to electronic excited state. All other transition

processes are omitted because of much smaller transition rates. The rate equation of the system can thus be written as:

$$\frac{dN_1}{dt} = W_{12}(N_2 - N_1) + w_{21}N_2 \quad \text{(M.1.1)}$$

$$\frac{dN_2}{dt} = W_{23}(N_3 - N_2) + W_{12}(N_1 - N_2) - w_{21}N_2 \quad \text{(M.1.2)}$$

$$\frac{dN_3}{dt} = W_{23}(N_2 - N_3) \quad \text{(M.1.3)}$$

We first consider the epr-SRS process for C≡N Raman mode in Rh800. The epr-SRS excitation probability at C≡N resonance is measured to be ΔI/I = 2×10^{-5} per pump pulse with 1-mM Rh800 DMSO solution, under 12-mW pump beam (838-nm) and 13-mW Stokes beam (1031.2-nm). With an 80-MHz repetition rate, one 2-ps pump pulse contains 6×10^8 photons at this power, which indicates 1.2×10^4 SRS transitions in one pulse duration. There are about 1.2×10^5 molecule in the focal volume with an N.A.=1.2 objective and 1-mM concentration (2.0×10^{-13} cm^3 focal volume [35]). Hence, the epr-SRS transition probability is about 0.1 per molecule per pulse under these conditions. Moreover, the transition rate for W_{12} is $1.2\times10^4/(1.2\times10^5\times2\times10^{-12}s)=5\times10^{10}$ per molecule per second (s) within the pulse duration. This represents an average epr-SRS transition rate of $5\times10^{10}/s\times2\times10^{-2}s\times80$ $MHz=8\times10^3$ per molecule per millisecond (ms). The linewidth of C≡N mode of Rh800 was measured to be 11 cm^{-1}, indicating a 0.5-ps lifetime (τ_{21}) [7]. Therefore, we have $w_{21}=2\times10^{12}$/s. The absorption cross-section for Rh800 at the peak absorption wavelength is 4×10^{-16} cm^2. Assuming a Franck-Condon factor of 0.1, a value reasonable for many electronic coupled vibrational modes[7], W_{23} is then $6\times10^8\times0.1\times4\times10^{-16}cm^2/(1.2\times10^{-9}cm^2\times2\times10^{-12}s)=10^{13}$ (focal area is $1.2\times10^{-9}cm^2$) per pulse duration (it should be noted that even the Franck-Condon factor is ten times smaller, the solution of equation (M.1.1-3) did not have obvious change). Obviously, because both probe process (time constant determined by W_{23}) and the SRS pumping process (time constant determined by w_{21}) have a time constant smaller than the laser pulse width, the steady state solution of equation (M.1.1-3) should be a good approximation,

$$N_3 = N_2 = N_1\frac{W_{12}}{w_{21} + W_{12}} \approx N_1\frac{W_{12}}{w_{21}} = \tau_{12}W_{12}N_1 \approx \tau_{12}W_{12}N \quad \text{(M.2)}$$

Note that W_{12} is much smaller than W_{23} here, hence, $N_1 \approx N$, the total molecule number in the laser focus. So, SREF emission rate, W_{SREF}, can be represent as,

$$W_{SREF} = f_{rep}N_3\eta = f_{rep}\tau_{12}W_{12}N\eta \propto f_{rep}\tau_{12}\sigma I_p I_s N\eta \quad \text{(M.3)}$$

where f_{rep} is the laser repetition rate; I_p and I_s are the beam intensities of pump laser and Stokes laser, respectively; σ is the (pre-resonance) spontaneous Raman cross section of the

C≡N Raman mode; η is the fluorescence quantum yield of Rh800. Equation (M.3) shows that the SREF signal is proportional to molecule concentration, Stokes beam intensity, Pump beam intensity, vibrational state lifetime, and laser repetition rate as long as the time interval between two adjacent pulses is longer than the fluorescence life time.

Under obtained parameters of W_{12}, w_{21}, W_{23}, we also numerically calculated the population dynamics of 50-μM Rh800 DMSO solution (6000 molecule at the focal volume) in one pulse duration of 2-ps. The readers can check that the result is very close to the steady state result (M.2). The initial populations at the beginning of the pulse are set to N_1=6000, N_2=N_3=0. Numerically solving the equation (M.1.1–3) within 2-ps pulse duration, the time-evolved solutions in Supplementary Fig. 4b show that both N_2 and N_3 reach about 120 at the end of the pulse. This result indicates that the probability for one molecule being excited to electronic transition state after one pulse excitation is 2% (=120/6000), corresponding to a single molecule SREF transition rate of 80000 pulses/ms×0.02 /pulse= 1600/ms. The coupling efficiency between epr-SRS and the probe process is hence $1600/8\times10^3$ = 20%. With a 16% fluorescence quantum yield [16] of Rh800 dye molecule and a collection efficiency ~ 2% of our microscope (estimated including all optics and electronic yield), the SREF signal size for one molecule equals to 80000×0.02×0.16×0.02≈5 photon/ms.

It is worth noting that, due to the sub-picosecond lifetime of vibrational relaxation, only a small portion of the SRS transitions can be successfully transferred as population at the electronic excited state, which contributes to SREF signal. Under steady state approximation, the coupling efficiency of the probing process can be simply represented as

$$\eta_c = \frac{N_3}{N_1 W_{12} \tau_{pulse}} = \frac{\tau_{12} W_{12} N_1}{N_1 W_{12} \tau_{pulse}} = \frac{\tau_{12}}{\tau_{pulse}} \quad \text{(M.4)}$$

Here τ_{pulse} is the pulse width. For our system, equation (M.4) gives 0.5ps/2ps = 25%, which is very close to the numerical simulation showed above. To increase the coupling efficiency without losing the spectral resolution, the shortest pulse for SREF excitation is around 1 ps for Fourier transform-limited pulse laser system (bandwidth ~10 cm^{-1}).

Experimental procedures for SREF spectroscopy and imaging.

Materials for sample preparation.—Dimethyl sulfoxide (DMSO) (Sigma, D8418), toluene (Sigma, 650579), Rhodamine 800 (Rh800) (Sigma, 83701), ATTO740 (ATTO-TEC, AD 740-21), PMMA (Electron Microscopy Sciences, PMMA powder in the kit, 14655), sulfate acid (Sigma, 258105), Hydrogen peroxide solution (30 wt. % in water) (Sigma, 216763).

Staining and imaging of living E. coli cells in Fig. 3.—Cells were incubated with 0.5 μM Rh800 in PBS for 15 min at room temperature for different isotopologues, then centrifuged and washed with PBS at room temperature before mixing together. After mixing, the cells were seeded on polylysine coated coverslip for SREF imaging. The pixel dwell time of galvanometer-driven raster scanning system was set to 10 μs. Nineteen-frame SREF image series were acquired by fixing the Stokes beam at 1,031.2 nm and scanning the

pump beam through 836.5-845.5 nm range with a 0.5-nm step size. P_{pump} and P_{Stokes} were 12 mW and 10 mW, respectively.

Single-molecule sample preparation.—PMMA solution (1 wt. % in toluene) was prepared by directly dissolving PMMA powder in toluene. 10-mM Rh800 DMSO solution was pre-diluted to 1-nM in toluene, and further diluted to 50-pM in above PMMA solution. Finally, the 50-pM Rh800 PMMA solution was spin-coated (5000 r/min, Laurell Technologies Corporation) onto a quartz coverslip (Alfa Aesar) to form PMMA-embedded single molecule specimen. Quartz coverslips were cleaned by first soaking in Piranha solution (H_2SO_4: H_2O_2 solution = 3:1 v/v) at 90 degrees Celsius overnight, and then by 30-min ultrasonic cleaning in deionized water for more than 4 times.

SREF spectroscopy and imaging of Rh800 and its isotopologues in Fig. 4.—For ensemble SREF spectra recording of Rh800 and its isotopologues in PMMA films, samples were prepared by spin-coating 500-nM corresponding dyes in 1% PMMA toluene onto quartz coverslips. P_{pump} and P_{Stokes} were 12 mW and 13 mW, respectively. For single-molecule SREF imaging shown in Fig. 4, the imaging sequence was initial fluorescence imaging (660-nm laser excited), sequential SREF spectral imaging series, and final fluorescence imaging again. Pixel size were set to 100-nm×100-nm; and pixel dwell time were set to 2-ms. P_{pump} and P_{Stokes} were 8 mW and 6 mW, respectively.

Single-molecule statistical analysis in Fig. 4.—For Student's t-test of 61 sets of single-molecule SREF images shown in Fig. 4, signals of 25 pixels in the 5×5-pixel center areas of corresponding images were used. p-values of on/off tests are the results of one-tailed paired t-tests between the on-resonance channel (Pump wavelength =838 nm) and adjacent two off-resonance channels (Pump wavelength =837 nm and 839 nm), respectively; the p-value of off/off control tests are the results of two-tailed paired t-test between the high-energy-side off-resonance channel (Pump wavelength = 837 nm) and the low-energy-side off-resonance channel (Pump wavelength = 839 nm). On/off ratios were calculated by dividing the on-channel signal by the average signal of adjacent two off-resonance channels.

Data availability

The data that support the plots within this paper and other findings of this study are available from the corresponding author upon reasonable request.

Supplementary Material

Refer to Web version on PubMed Central for supplementary material.

Acknowledgements:

We are grateful for the discussion with L. E. Brus and X.Y. Zhu. This work was supported by grant of R01GM128214 from NIH, and by the Camille and Henry Dreyfus Foundation.

References:

1. Lakowicz JR Principles of Fluorescence Spectroscopy. 3 edn, (Springer US, New York, 2007).

2. Moerner W & Orrit M Illuminating single molecules in condensed matter. Science 283, 1670–1676 (1999). [PubMed: 10073924]
3. Schatz GC & Ratner MA Quantum Mechanics in Chemistry. (Courier Corporation, New York, 1993).
4. Herzberg G Infrared and Raman Spectra of Polyatomic Molecules. Vol. 2 (D. Van Nostrand Company, New York, 1945).
5. Nie S & Emory SR Probing single molecules and single nanoparticles by surface-enhanced Raman scattering. Science 275, 1102–1106 (1997). [PubMed: 9027306]
6. Seilmeier A, Kaiser W, Laubereau A & Fischer S A novel spectroscopy using ultrafast two-pulse excitation of large polyatomic molecules. Chemical Physics Letters 58, 225–229 (1978).
7. Hübner H-J, Wörner M, Kaiser W & Seilmeier A Subpicosecond vibrational relaxation of skeletal modes in polyatomic molecules. Chemical physics letters 182, 315–320 (1991).
8. Mastron JN & Tokmakoff A Two-photon-excited fluorescence-encoded Infrared spectroscopy. The Journal of Physical Chemistry A 120, 9178–9187 (2016). [PubMed: 27802385]
9. Cheng J & Xie X Coherent anti-Stokes Raman scattering microscopy: Instrumentation, theory, and applications. Journal of Physical Chemistry B 108, 827–840 (2004).
10. Min W, Freudiger CW, Lu S & Xie XS Coherent nonlinear optical imaging: beyond fluorescence microscopy. Annual review of physical chemistry 62, 507–530 (2011).
11. Lee S, Nguyen D & Wright J Double resonance excitation of fluorescence by stimulated Raman scattering. Applied Spectroscopy 37, 472–474 (1983).
12. Shim S, Stuart CM & Mathies RA Resonance Raman cross-sections and vibronic analysis of Rhodamine 6G from broadband stimulated Raman spectroscopy. ChemPhysChem 9, 697–699 (2008). [PubMed: 18330856]
13. Wei L & Min W Electronic preresonance stimulated Raman scattering microscopy. The Journal of Physical Chemistry Letters 9, 4294–4301, doi:10.1021/acs.jpclett.8b00204 (2018). [PubMed: 30001137]
14. Etchegoin PG, Le Ru EC & Meyer M Evidence of natural isotopic distribution from single-molecule SERS. Journal of the american chemical society 131, 2713–2716 (2009). [PubMed: 19166340]
15. Min W et al. Imaging chromophores with undetectable fluorescence by stimulated emission microscopy. Nature 461, 1105–1109 (2009). [PubMed: 19847261]
16. Sperber P, Spangler W, Meier B & Penzkofer A Experimental and theoretical investigation of tunable picosecond pulse generation in longitudinally pumped dye laser generators and amplifiers. Optical and quantum electronics 20, 395–431 (1988).
17. Wei L et al. Super-multiplex vibrational imaging. Nature 544, 465–470 (2017). [PubMed: 28424513]
18. Dean KM & Palmer AE Advances in fluorescence labeling strategies for dynamic cellular imaging. Nature chemical biology 10, 512–523 (2014). [PubMed: 24937069]
19. Kneipp K et al. Single molecule detection using surface-enhanced Raman scattering (SERS). Physical review letters 78, 1667–1670 (1997).
20. Sonntag MD et al. Single-molecule tip-enhanced Raman spectroscopy. The Journal of Physical Chemistry C 116, 478–483 (2011).
21. Yampolsky S et al. Seeing a single molecule vibrate through time-resolved coherent anti-Stokes Raman scattering. Nature Photonics 8, 650–656 (2014).
22. Zhang Y et al. Coherent anti-Stokes Raman scattering with single-molecule sensitivity using a plasmonic Fano resonance. Nature communications 5, 4424 (2014).
23. Mahmoudi M et al. Protein− nanoparticle interactions: opportunities and challenges. Chemical reviews 111, 5610–5637 (2011). [PubMed: 21688848]
24. Macklin J, Trautman J, Harris T & Brus L Imaging and time-resolved spectroscopy of single molecules at an interface. Science 272, 255–258 (1996).
25. Nie S, Chiu DT & Zare RN Probing individual molecules with confocal fluorescence microscopy. Science 266, 1018–1021 (1994). [PubMed: 7973650]

26. Kukura P, Celebrano M, Renn A & Sandoghdar V Single-molecule sensitivity in optical absorption at room temperature. The Journal of Physical Chemistry Letters 1, 3323–3327 (2010).
27. Chong S, Min W & Xie XS Ground-state depletion microscopy: detection sensitivity of single-molecule optical absorption at room temperature. The Journal of Physical Chemistry Letters 1, 3316–3322 (2010).
28. Gaiduk A, Yorulmaz M, Ruijgrok P & Orrit M Room-temperature detection of a single molecule's absorption by photothermal contrast. Science 330, 353–356 (2010). [PubMed: 20947760]
29. Zrimsek A et al. Single-molecule chemistry with surface-and tip-enhanced Raman spectroscopy. Chemical reviews 117, 7583–7613 (2017). [PubMed: 28610424]
30. Winterhalder M, Zumbusch A, Lippitz M & Orrit M Toward far-field vibrational spectroscopy of single molecules at room temperature. The Journal of Physical Chemistry B 115, 5425–5430 (2011). [PubMed: 21381637]
31. Brinks D et al. Ultrafast dynamics of single molecules. Chemical Society Reviews 43, 2476–2491 (2014). [PubMed: 24473271]
32. Kukura P, McCamant DW & Mathies RA Femtosecond stimulated Raman spectroscopy. Annu. Rev. Phys. Chem 58, 461–488 (2007). [PubMed: 17105414]
33. Siegman AE Lasers. (University Science Books, Mill Valey, CA, 1986).
34. Wright JC Double resonance excitation of fluorescence in the condensed phase—an alternative to Infrared, Raman, and fluorescence spectroscopy. Applied Spectroscopy 34, 151–157 (1980).
35. Zipfel WR, Williams RM & Webb WW Nonlinear magic: multiphoton microscopy in the biosciences. Nature biotechnology 21, 1369–1377 (2003).

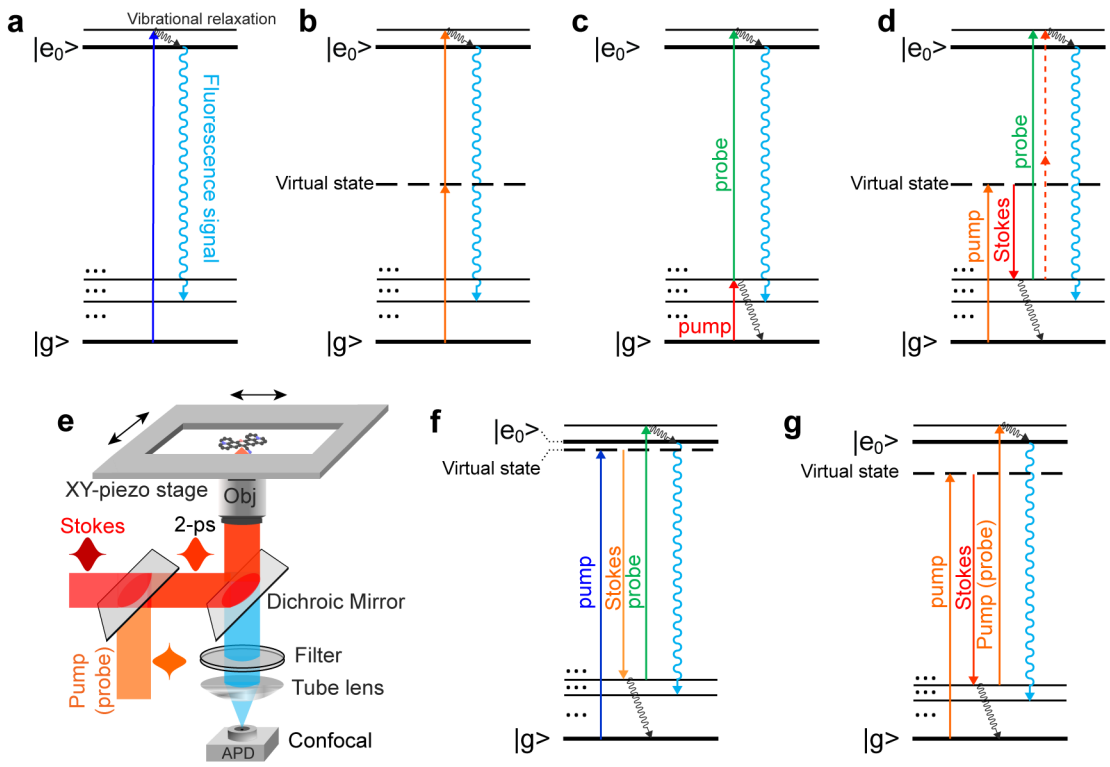

Fig.1 |. Encoding vibrational features into fluorescence spectroscopy.

Energy diagrams of (**a**) one-photon excited fluorescence; **b**, conventional two-photon excited fluorescence; **c**, Infrared-mediated double-resonance fluorescence; **d**, stimulated Raman excited fluorescence (SREF); **e**, Experimental setup for this research (details in Methods). Temporally and spatially overlapped pump (probe) and Stokes pulse trains (2 picosecond, 80 MHz) are focused by a high N.A. objective. Backward emitting fluorescence is then detected by an APD for confocal detection; **f**, SREF with rigorous/close electronic resonance for the SRS process; **g**, SREF with proper electronic pre-resonance for the SRS process.

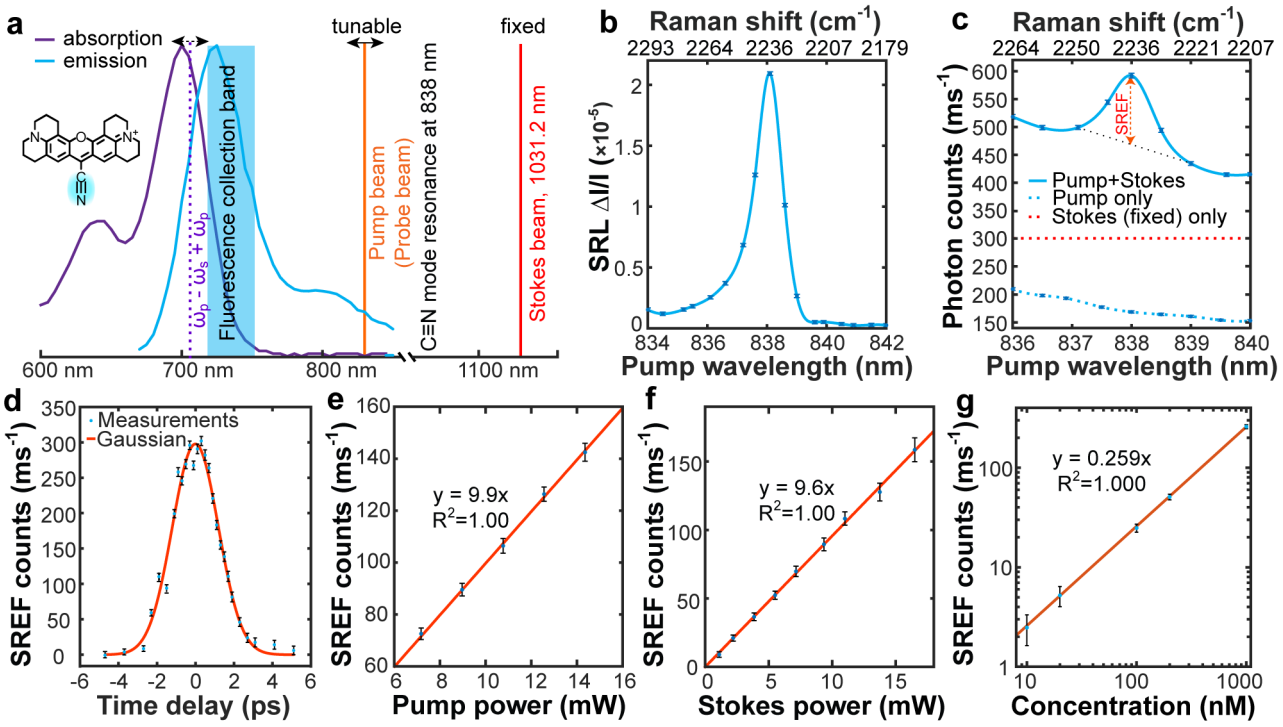

Fig.2 |. Stimulated Raman excited fluorescence (SREF) spectroscopy.

a, SREF experimental scheme on Rhodamine 800 (Rh800). Absorption (purple) and emission (blue) spectra of Rh800 in DMSO are shown, together with the tunable pump beam (orange), the fixed Stokes beam at 1031.2-nm (red) and the energy level of $(\omega_p - \omega_s) + \omega_p$ (purple dash). Pump beam is also used as the probe beam. **b**, SRS spectrum for C≡N vibration of 1-mM Rh800 solution in DMSO. **c**, SREF excitation spectrum of 500-nM Rh800 solution in DMSO (blue solid). Pure SREF signal size is indicated. Pump-only (blue dash) and Stokes-only (red dash) excitation results are also shown. **d**, Pure SREF signal as a function of the relative time delay between pump and Stokes pulses. **e**, Pump-power dependence of pure SREF signal. Stokes power set to 6 mW. **f**, Stokes-power dependence of pure SREF signal. Pump power set to 6 mW. **g**, Dependence of pure SREF signals on Rh800 concentrations in DMSO. In **b**, **c**, **d** and **g**, P_{pump} and P_{Stokes} are 12 mW and 13 mW, respectively. From **b** to **g**, the error bars represent 95% confidence intervals of the mean values of normal distributions fitted by 100 independent measurements, respectively.

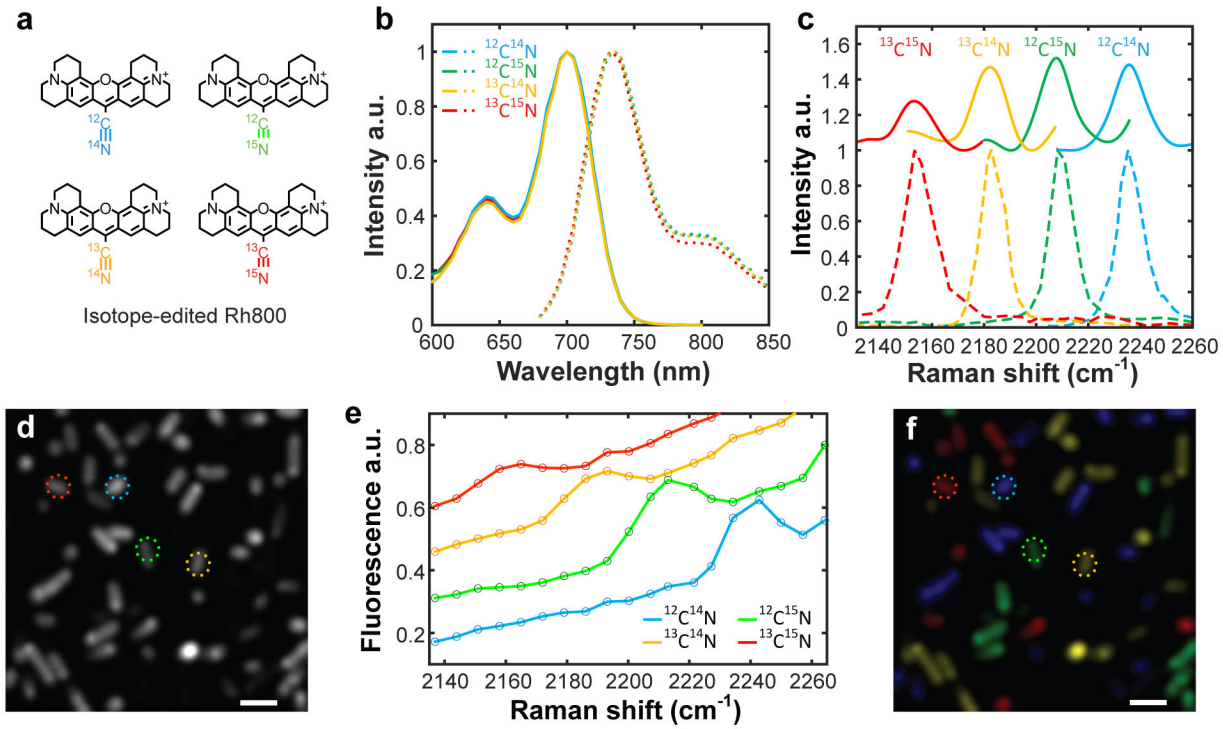

Fig. 3 |. Living-cell multicolor SREF microscopy.

a, Chemical structures of Rh800 and its three derivatives with isotopically-edited nitrile bonds. **b**, Absorption and emission spectra for four Rh800 isotopologues. **c**, SREF excitation spectra (color-coded solid lines) and the corresponding SRS spectra (color-coded dash lines) for four Rh800 isotopologues in DMSO. **d**,**f**, Fluorescence imaging (**d**) and multicolor SREF imaging (**f**) of living *E. coli* stained by four Rh800 isotopologues. **e**, SREF spectra of cells marked by corresponding circles in **d** and **f**. In **f**, colors are manually coded by corresponding SREF spectra. Scale bars: 2 μm.

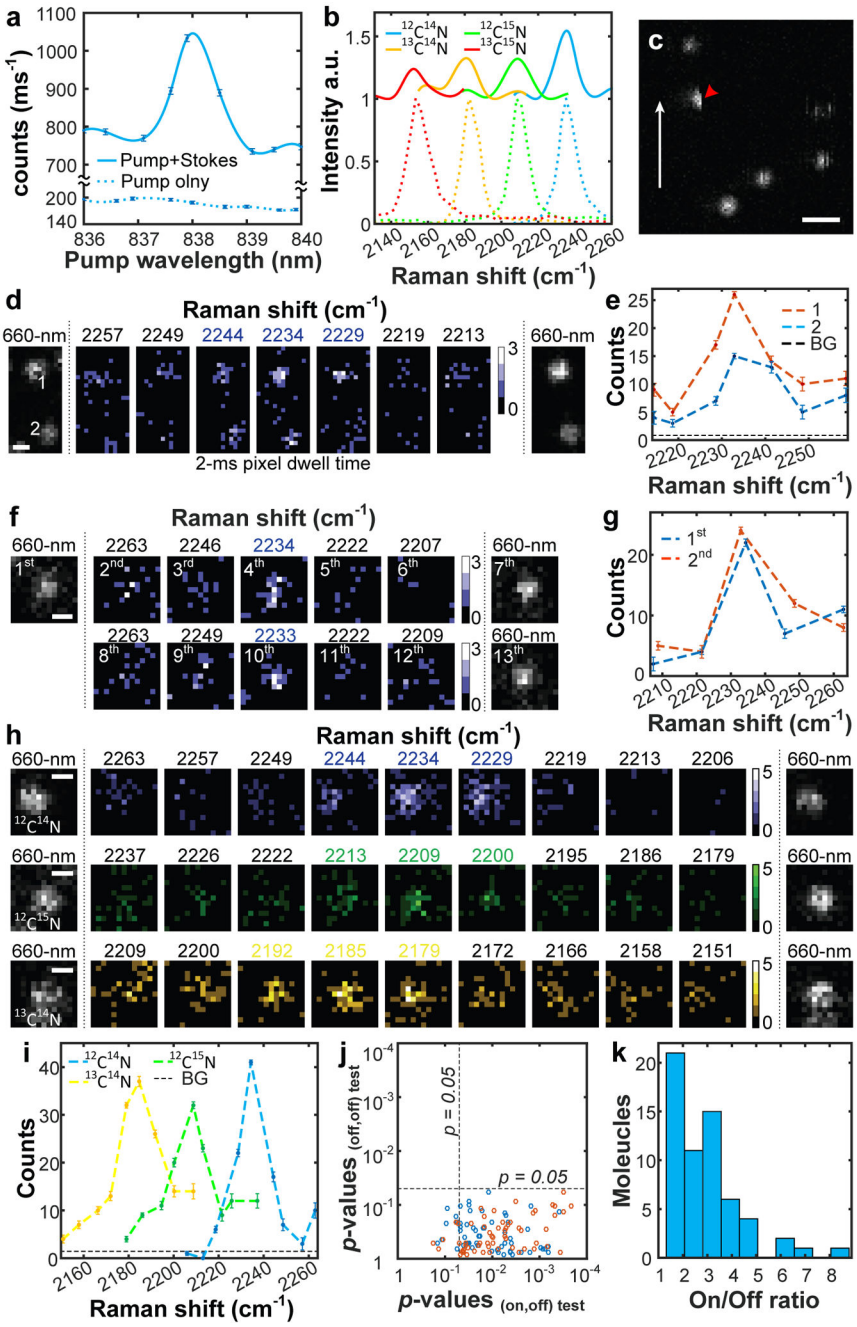

Fig. 4 |. Single-molecule SREF spectroscopy and imaging.

a,**b**, Ensemble SREF excitation spectra of Rh800 (**a**) and its isotopologues (**b**) in PMMA films. Color-coded dash lines in (**b**) show corresponding SRS spectra. **c**, Single-molecule fluorescence image excited by 660-nm CW laser. White arrow shows fast axis of raster scanning. Red arrow indicates 'half-moon' photobleaching. Scale bar, 1-μm. **d**,**e**, Recording single-molecule SREF spectra of two Rh800 molecules simultaneously (red dash, molecule 1; blue dash, molecule 2). **f**,**g**, Recording SREF spectra of the same molecule by two rounds (blue dash, the first round; red dash, the second round). **h**,**i**, Single-molecule SREF images

of Rh800 isotopologues. In **d**, **f** and **h**, color bars, counts per 2-ms; scale bars: 400-nm. In **e**, **g** and **i**, photon counts are the sum of photons within the 5×5-pixel center areas of corresponding images; BG (background) and error bars are the average and standard deviation of photon counts of nearby 50 molecule-free 5×5-pixel regions, respectively. **j**, Student's t-test of signals between the on-resonance channel and its adjacent two off-resonance channels (blue and red circles, respectively), and between the two off-resonance channels for 61 sets of single-molecule SREF images. **k**, On/Off ratio distribution of the 61 sets.